The *Drosophila lethal(2)giant larvae* Tumor Suppressor Protein Is a Component of the Cytoskeleton

Dennis Strand, Ivan Raska,* and Bernard M. Mechler

Department of Developmental Genetics, Deutsches Krebsforschungszentrum, D-69120, Germany; and * Academy of Sciences of the Czech Republic, Institute of Experimental Medicine, 12800 Prague 2, Czech Republic

Abstract. Tumor suppressor genes act as recessive determinants of cancer. In *Drosophila* these genes play a role in normal development and are essential for regulating cell growth and differentiation. Mutations in the gene, *lethal(2)giant larvae, l(2)gl*, besides causing malignant tumors in the brain and imaginal discs, generate developmental defects in a number of other tissues. Much of the uncertainty regarding the function of the *l(2)gl* gene product, p127, results from a lack of knowledge as to the precise location of this protein in the cell. We have investigated the cellular and subcellular localization of p127, using confocal and electron microscopy as well as biochemical and cell fractionation procedures. Our analyses indicate that p127 is located entirely within the cell in both the cytoplasm and bound to the inner face of lateral cell membranes in regions of cell junctions. On the membrane, p127 can form large aggregates which are resistant to solubilization by nonionic detergents, indicating that p127 is participating in a cytoskeletal matrix. These findings suggest that the changes in cell shape and the loss of apical–basal polarity observed in tumorous tissues are a direct result of alterations in the cytoskeleton organization caused by *l(2)gl* inactivation and also suggest that p127 is involved in a cytoskeletal-based intercellular communication system directing cell differentiation.

T HE *lethal(2)giant larvae, (l(2)gl)*, gene is one of a growing number of genes identified in *Drosophila* that control cell proliferation and differentiation (Gateff and Mechler, 1989; Mechler and Strand, 1990; Mechler, 1991; Török et al., 1993*b*). When both copies of these genes are inactivated cell proliferation becomes unrestricted and cell differentiation is arrested. These *Drosophila* genes exhibit similar characteristics to human tumor suppressor genes. However, while so far no *Drosophila* tumor suppressor gene has been identified as a human tumor suppressor gene (for review see Knudson, 1993), recent molecular analyses have shown that several *Drosophila* tumor suppressor genes display sequence similarity with mouse or human genes whose involvement in vertebrate carcinogenesis has yet to be demonstrated (Bryant and Woods, 1992; Cho et al., 1992; Watson et al., 1992; Stewart and Denell, 1993; Tomotsune et al., 1993). Furthermore, it has been shown that the human tumor suppressor gene, APC, is associated with β-catenin (Rubinfeld et al., 1993; Su et al., 1993), for which the *Drosophila* homolog is the *armadillo* gene, a putative adherens junction protein and a key player in the *wingless* signaling pathway (Peifer et al., 1993). Future studies into the function of the human and *Drosophila* genes should produce valuable insights into the control of cell growth and the mechanisms by which cells differentiate in both of these organisms.

Homozygous mutations in *l(2)gl* result in overgrowth of the optic lobes in the larval brain as well as overgrowth of the imaginal discs which coalesce into disorganized masses. Histology reveals that the brain tumors are made of undifferentiated neuroblasts and ganglion mother cells whereas the tumors of the imaginal discs consist of amorphic masses of cuboidal cells which have lost their characteristical apical–basal cell polarity and are unable to differentiate (Gateff and Schneiderman, 1969, 1974). Transplantation of *l(2)gl* brain or imaginal disc tumors into the abdomen of adult flies results in massive overgrowth of the implants with subsequent invasion of the host tissues. Recent data suggest that the invading cells undergo further changes that facilitate their invasiveness and indicate that *Drosophila* mutants affecting tumor suppressor genes can provide a simplified model system for studying metastasis (Timmons et al., 1993; Woodhouse et al., 1994).

Although the tumorous phenotype is clearly the most striking aspect of the inactivation of *Drosophila* tumour suppressor genes, other critical cellular functions may be impaired. In *l(2)gl*-deficient animals, abnormal development of several tissues such as the male germ cells (Hadorn and Gloor, 1942; Gloor, 1943), the ring gland (Hadorn, 1937; Scharrer and Hadorn, 1938; Aggarwal and King, 1969), and

the imaginal discs (Hadorn, 1938; Grob, 1952) is already discernable in either first or second instar larvae. Remarkably the overgrowth of the imaginal discs and the brain hemispheres becomes only apparent during the prolonged larval life of the mutant larvae (Gateff and Schneiderman, 1969), although growth abnormalities in these tissues can be histologically detected from the onset of the second larval instar (Gateff and Schneiderman, 1969). Moreover, the critical phase for commitment to tumorigenic growth can be traced back to early embryogenesis (Gateff and Schneiderman, 1974; Merz et al., 1989).

The *l(2)gl* gene encodes an 1,161-amino acid polypeptide of ~127 kD in molecular weight, designated as p127 (Jacob et al., 1985). Sequence comparison of *l(2)gl* orthologues in other *Drosophila* and diptera species (Török et al., 1993a) reveals the presence of conserved domains which may represent important functional domains within the p127 protein. Several of these domains are also conserved in the recently isolated mouse homolog to *l(2)gl* (Tomotsune et al., 1993). None of the conserved sequences appears to be a membrane-spanning sequence, suggesting that these proteins are intracellular rather than transmembrane or extracellular proteins. Previous sequence analyses have assigned cell adhesion properties in the *l(2)gl* gene product with similarities to either neural cell adhesion molecule (N-CAM)[1] (Lützelschwab et al., 1987) or liver cell adhesion molecule (L-CAM) (Klämbt et al., 1989), although biochemical data supporting or refuting this assumption have been lacking (Hortsch and Goodman, 1991).

Since no conclusive information on a possible function of *l(2)gl* could be gained from examination of the encoded protein sequence, we have investigated the cellular and subcellular distribution of p127 throughout *Drosophila* development. The knowledge of the precise subcellular localization of p127 is a prerequisite for elucidating the function of this protein. In this paper we show that p127 is located entirely within the cell, either dispersed in the cytoplasm or bound to the internal face of the plasma membrane. Moreover, p127 displays characteristics of a cytoskeletal or cytoskeleton-associated protein particularly when it is bound to the plasma membrane. These findings support the view that the changes in cell shape and the loss of cell polarity in *l(2)gl* tumorous cells may directly result from alterations in the organization of the cytoskeleton induced by the absence of p127.

Materials and Methods

Antibodies

Peptides corresponding to the NH₂- and COOH-terminal ends of the p127 protein with the sequence LKFIRGKGQQPSADRHRLQKDC and CHE-KTNGDNKIGTPKTAPEESQF, respectively, were conjugated to maleimide activated keyhole limpet hemocyanin (Pierce Chemical Co., Rockford, IL) through the terminal cysteine of each peptide and the resulting conjugates were used to immunize rabbits. Anti–peptide antibodies were purified as described by Harlow and Lane (1988) by affinity chromatography on columns of protein A, followed by affinity chromatography on columns of the immunizing peptide coupled to Sulfo-link coupling gel (Pierce Chemical Co.). Antibodies to a central portion of p127 (amino acids 59–463), designated pEX215, were obtained by fusing this region to β-galactosidase in the pEX expression vector (Boehringer Mannheim

---

1. *Abbreviations used in this paper*: N- and L-CAM, neural and liver cell adhesion molecule; S, supernatant; P, pellet.

GmbH, Mannheim, Germany) and injecting the fusion proteins into rabbits. Antibodies were purified by first passing the immune serum over a column of β-galactosidase coupled to Sepharose followed by affinity chromatography on columns of the pEX215 fusion protein coupled to Sepharose. The specificity of the purified antibodies was controlled by performing immunostaining of normal and *l(2)gl* mutant tissues, as well as by immunoblots of protein extracts. In addition, the specificity of the anti–peptide antibodies was controlled by immunostaining and immunoblotting in the presence of excess peptide (100 μg/ml) (see Fig. 1). Texas red-conjugated goat anti-rabbit antibodies were obtained from Dianova GmbH (Hamburg, Germany). Secondary antibodies for Western blotting were either gold labeled (Immunogold system; Amersham Corp., Arlington Heights, IL) or coupled to alkaline phosphatase (Tropix system; Serva, Heidelberg, Germany) and used as recommended by the manufacturers. Phalloidin-FITC and anti-actin antibodies were obtained from Sigma Chemical Co. (St. Louis, MO).

Indirect Immunofluorescence Staining of Whole-mount Fixed Embryos and Tissues

Standard techniques for removing the vitelline membrane, fixing the embryos, and antibody staining were used throughout (Ashburner, 1989). Embryos from *Drosophila melanogaster* (Oregon R strain) were collected at 25°C, gently rinsed off the plates, and dechorionated in 3% Na-hypochlorite solution for 90 s. After extensive washing, the dechorionated embryos were fixed and the vitelline membrane removed by 15 min of shaking in 3 ml of a 1:1 solution of heptane/4% paraformaldehyde solution. The lower layer of fixative was removed and replaced with 4% paraformaldehyde in PBS plus 0.1% sodium deoxycholate and 0.1% Triton X-100 and the incubation with constant shaking was continued for 15 min. The lower PBS phase was removed completely, 3 ml of absolute methanol were added and the tube was vigorously shaken. All heptane and methanol was removed and the embryos rehydrated by passage into PBS, before blocking in 3% BSA and 3% goat serum in PBS for at least 1 h at room temperature. The blocking solution was removed and antibodies were added at a concentration of 5–10 μg/ml in blocking solution for 2 h at room temperature or overnight at 4°C. After three successive washes in PBS for 1 h or longer, the embryos were stained for 1 h with goat anti-rabbit IgG coupled to Texas red (Dianova). After a 1 h washing in PBS, the embryos were mounted in elvanol for microscopic evaluation using a Zeiss LSM microscope.

For examination of larval and adult tissues, the tissues were first dissected in *Drosophila* Ringer's solution and then fixed for 15 min in 4% paraformaldehyde in PBS. All subsequent antibody incubations were the same as for embryos.

Isolation of Primary Drosophila Embryonic Cells

Primary embryonic cells from gently homogenized embryos were isolated by velocity sedimentation through discontinuous metrizamide (grade II; Sigma Chemical Co.) gradients. Briefly, ~1 g of dechorionated embryos were homogenized in 20 ml of BSS (Ashburner, 1989) by three to five gentle strokes of a loose fitting pestle in a 40 ml Dounce homogenizer. The homogenate was filtered through two layers of Nitex screen ~300 and 100 μm mesh and the screen washed with an additional 10–20 ml of BSS. Cells were pelleted at 200 g for 10 min at 4°C, washed in 10 ml BSS, pelleted again, and resuspended in 0.5 ml BSS before layering on the top of a metrizamide gradient consisting of 2 ml steps of 30, 20, and 5% metrizamide in BSS in a 15 ml centrifuge tube. The gradient was centrifuged in a swinging bucket rotor at 4°C for 30 min at 750 g and the cells collected from the 5–20% interface in a volume of ~0.5 ml which was transferred into a 2 ml centrifuge tube and diluted slowly with 1.5 ml BSS before pelleting at 200 g. The resulting cell pellet was resuspended in an appropriate medium or buffer for further analysis. Using this procedure, typically, 4 × 10⁷ cells/g of embryos were isolated with >90% viability as determined by Trypan blue exclusion.

Trypsin Digestion

For trypsin digestion experiments, primary embryonic cells were prepared as above and resuspended in BSS at a density of 4 × 10⁷ cells/ml. 2 × 10⁶ cells in a volume of 50 ml or Triton X 100 extracts of an equal number of cells in the same volume were dispensed and trypsin was added to the indicated concentration. When indicated soybean trypsin inhibitor was added to 200 μg/ml before trypsin addition and was also used to terminate all reactions after 15 min at room temperature. Cells were pelleted and lysed in

2× Laemmli sample buffer, whereas the detergent extracts were directly processed into 2× sample buffer. All samples were boiled for 5 min and the proteins separated on 7% SDS-PAGE gels, followed by Western blot analysis.

Topological Analysis by Antibody Staining

Spodoptera frugiperda (Sf9) cells infected with recombinant baculoviruses containing the *l(2)gl* cDNA sequence coding for p127 (Sf9:p127) were grown in six-well tissue culture dishes for 32 h after infection. After removal of the tissue culture medium the cells were washed once with PBS and then fixed in PLP fix (2% paraformaldehyde, 0.2 M lysine, 0.1 M sodium periodate in 0.1 M sodium phosphate buffer, pH 7.4) for 10 min at room temperature. Fixative was removed and the cells were washed three times with PBS. Primary antibodies in 3% BSA in PBS were added for 2 h with and without addition of 0.1% saponin as indicated. After three washes in PBS, the cells were incubated for 2 h with Texas red coupled goat anti-rabbit antibodies. The stained cells were washed three times in PBS and mounted on microscope slides.

Surface Biotinylation

Sf9 cells (2 × 10^6 cells/ml) infected with recombinant *l(2)gl* baculoviruses were washed three times in PBS, pH 8.0, and were either incubated in the tissue culture dish with 2 mg/ml sulfosuccinimidyl 6-(biotinamido) hexanoate (NHS-LC-biotin; Pierce Chemical Co.) for surface labeling or harvested and extracted in 1% NP-40/PBS, pH 8.0, followed by addition of NHS-LC-biotin to 2 mg/ml for total protein labeling. After incubation for 1 h at 4°C with gentle rocking, the surface-labeled cells were washed three times with PBS, harvested, and lysed in 1% NP-40/PBS. After clearing of the extract from an equivalent of 2 × 10^6 cells at 13,000 g for 10 min at 4°C, p127 was immunoprecipitated with 20 µg anti-peptide antibody and 25 µl protein A-Sepharose (Boehringer Mannheim GmbH) overnight at 4°C. In the case of the detergent extracts exposed to NHS-LC-biotin, 1 M Tris, pH 8.0, was added to 50 mM and the incubation continued for 15 min before clearing at 13,000 g for 10 min at 4°C. The supernatant was immunoprecipitated as described above. Immunoprecipitates were washed three times with 1% NP-40/PBS before addition of 100 µl of 2× sample buffer and boiled for 5 min. Each sample was identically loaded twice (40 µl/lane) onto two 7% SDS-PAGE gels. The proteins were transferred onto polyvinylidene difluoride (PVDF) membranes (Millipore Corp., Milford, MA). Identical blots were either probed with anti-peptide antibodies for p127 or for biotinylation using avidin-gold reagent and silver enhancement (Amersham Corp.).

Cell Fractionation

Wild-type embryos were disrupted in PBS using a tight fitting Dounce homogenizer. After low-speed centrifugation, 600 g for 15 min, to remove nuclei and debris, the resulting supernatant was used to generate a soluble (S-100) and a particulate (P-100) fraction by centrifuging at 100,000 g for 1 h at 4°C. The low-speed pellet containing nuclei, debris, and undisrupted embryos was further centrifuged through a 1.2 M sucrose cushion to purify the nuclear fraction.

Fractionation of embryonic extracts was performed by centrifugation on discontinuous sucrose density gradient according to the procedure of Mechler and Rabbits (1981). 2 g of embryos were homogenized in 3 ml TKM (50 mM Tris, pH 7.5, 150 mM KCl, 5 mM MgCl₂) with 10 strokes of a loose fitting pestle in a 20 ml Dounce homogenizer. The homogenate was passed through a 500 µm Nitex screen to remove debris and 2.0 ml filtrate was mixed with 12.5 ml of 2.5 M sucrose solution in TKM. This was layered below a step gradient of 10 ml 2.0 M sucrose and 5 ml of 0.5 M sucrose in TKM in a Beckman SW27.1 rotor centrifuge tube. After 2.5-h centrifugation at 24,000 rpm, the 0.5/2 M gradient interface (membrane fraction), the lower phase of sample plus 2.5 M sucrose (cytosolic), and pellet (nuclear) were collected. The membrane vesicles were sedimented at 5,000 g for 10 min after adding 2 vol TKM and the resulting pellets gently resuspended in 0.5 ml of the appropriate buffer for further analysis. The purity of the cellular fractions was monitored by light and electron microscopy.

Treatment of Membrane Fraction and Sf9:p127 Cells with Solubilizing Agents

The membrane fraction prepared as above was dispensed in 100-µl aliquots and pelleted. The pellet was resuspended in 1 ml of the various solubilizing
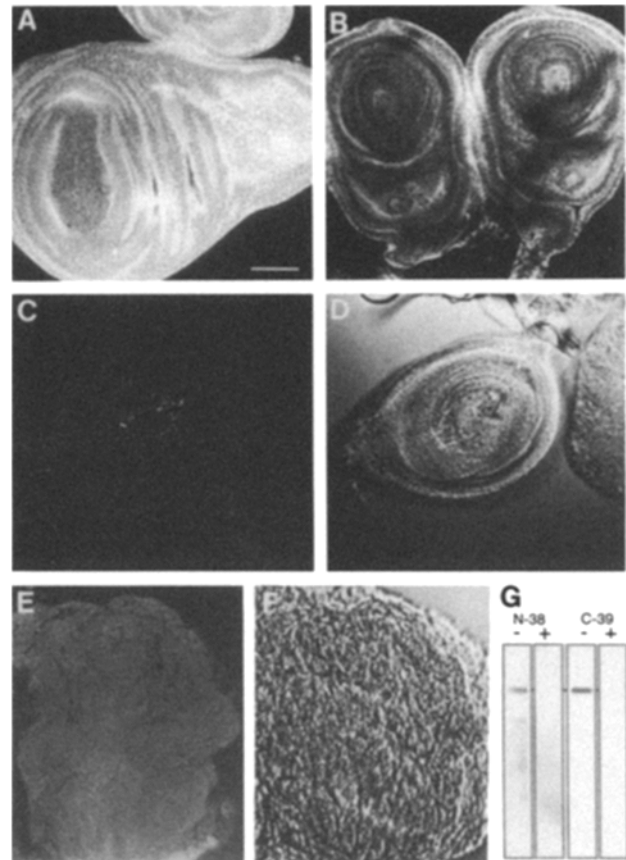

Figure 1. Specificity of anti-p127 antibodies. Confocal images of dissected third instar larvae tissues of wild type (*A–D*) or *l(2)gl* mutant imaginal disc tumours (*E* and *F*), stained with anti-p127 affinity purified C-39 antibodies (*A* and *B*) or with anti-p127 antibodies plus the addition of 100 µg/ml of the synthetic peptide used for immunization (*C* and *D*). *D* and *F* are differential interference contrast images of *C* and *E*. All fluorescent images were processed under identical conditions. (*G*) Western blots of total embryonic proteins developed with affinity-purified anti-peptide antibodies (*N-38* or *C-39*, see Materials and Methods for a description of the peptides) used for the immunocytochemistry in the absence (−) or presence (+) of excess peptides. Lines between panels mark the position of p127. Bar, 50 µm.

agents and incubated 30 min at room temperature. The reagents were as follows: PBS(control), 1% SDS, 1% NP-40, 100 mM glycine (pH 2.8), 50 mM ethanolamine (pH 11.5), 6 M urea, and 1 M NaCl. The suspensions were centrifuged at 13,000 g for 10 min at 4°C and the pellets solubilized in 2× sample buffer for 7% SDS-PAGE and Western blot analysis. The supernatants were added directly to 2× sample buffer and analysed in parallel.

For detergent extraction a membrane fraction isolated from 1 g of *Drosophila* embryos was suspended in 0.5 ml 1% NP-40/PBS solution for 10 min at 4°C followed by centrifugation at 13,000 g for 10 min at 4°C. The supernatant (S1) was removed and the pellet resuspended in 500 µl of NP-40 solution by gentle homogenization with a loose fitting pestle in a 2 ml Dounce homogenizer. The suspension was again centrifuged as before and the supernatant removed (S2). The pellet was processed as above through two further cycles before being completely solubilized in 2× sample buffer and analyzed by SDS-PAGE/Western procedures.

For in situ detection of p127 and actin, Sf9:p127 cells were grown on poly-L-lysine-coated coverslips for 36 h after infection. After removing medium, cells were washed with PBS and incubated in cold 0.2% NP-40 in PBS for 15 min followed by fixation in 4% paraformaldehyde for 10 min. Blocking in 3% BSA in PBS for 30 min preceded overnight incubation at 4°C with primary anti-peptide antibodies. The cells were washed three times in PBS and the incubation was continued for 2 h with goat anti-rabbit
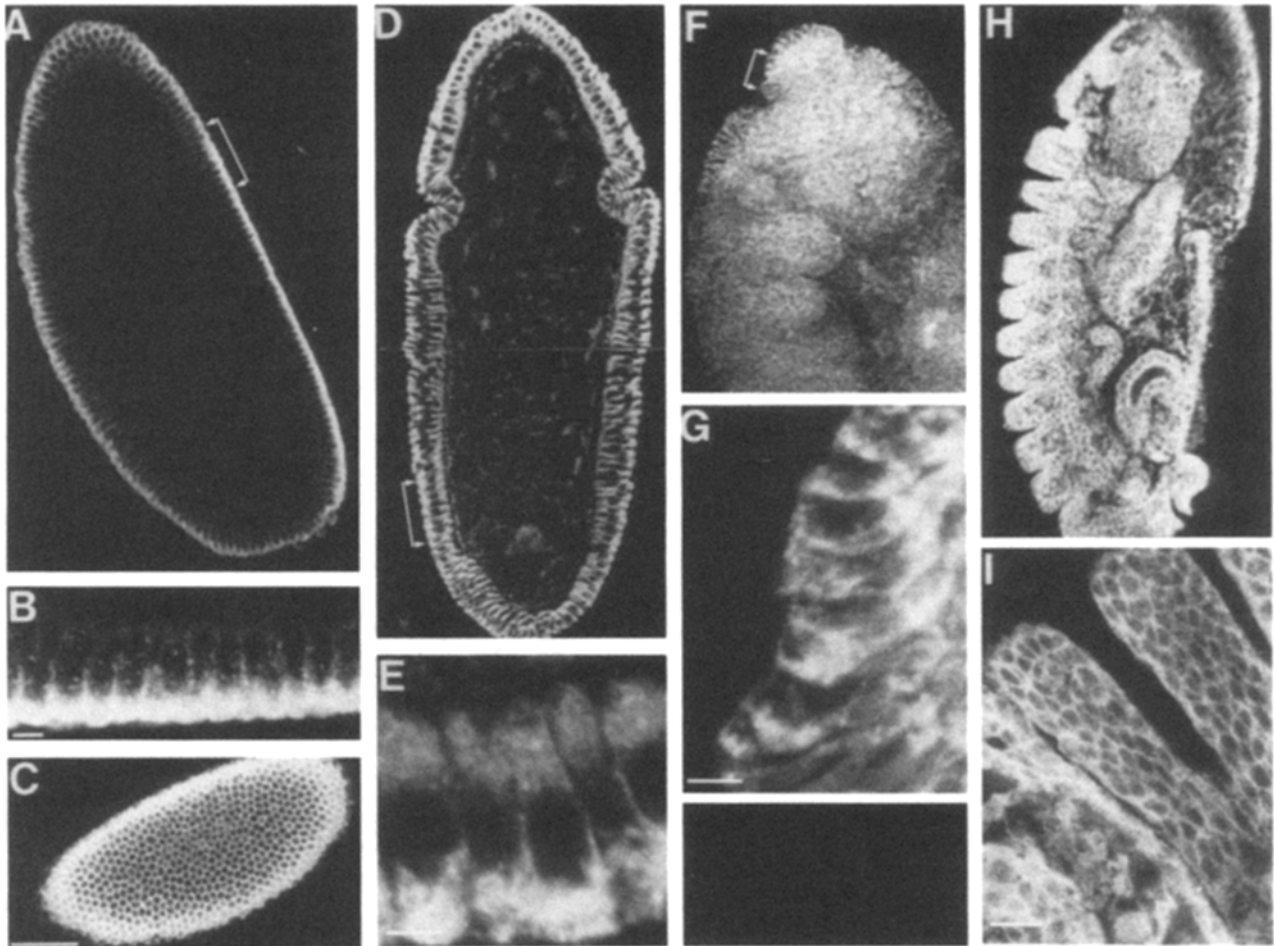
Figure 2. Ubiquitous expression of p127 during embryogenesis. Confocal microscope images of whole mount, wild-type embryos, fixed and stained with anti–p127 affinity purified antibodies. (*A–C*) Cellularizing blastoderm embryo showing staining in the apical periplasm and along the growing furrow canals. Note punctate staining in cytoplasm in *B*. (*C*) Tangential section of the embryo shown in *A*. Cell contacts are outlined. (*D* and *E*) Early stages of gastrulation. Staining is observed in periplasm and cell contact regions. Although some staining is visible in the basal portion of the cells, there is no staining of the basal cell membrane. (*F* and *G*) Extended germ band. Staining appears more diffuse at this stage. (*H* and *I*) Late stage of embryogenesis. Staining in epidermis and digestive tract as well as presumptive optic lobe is visible. *B*, *E*, and *G* are higher magnifications of the regions indicated by white brackets in *A*, *D*, and *F*, respectively. C-39 antibodies were used for all preparations shown in this figure. Bars: (*C*) 50 μm; (*I*) 10 μm; (*B, E*, and *G*), 5 μm.

Texas red conjugates and phalloidin–FITC. Coverslips with the stained cells were washed three times before mounting and viewing for confocal laser microscopy.

Expression of p127 from Baculoviruses in Sf9 Cells

To clone the p127 coding region into the baculovirus transfer vector pEV55, the entire 5.4-kb EcoRI fragment of cDNA clone Ecl73 (Jacob et al., 1987) was ligated into the transfer vector pEV55 (O'Reilly et al., 1992) previously digested with EcoRI. Recombinant baculoviruses were recovered by standard methods as described in Summers and Smith (1987) and O'Reilly et al. (1992). Sf9 cells were infected from virus stocks whose titers were determined by infecting 1×10^6 cells per well of a six-well culture dish with increasing amounts of virus. The minimum amount of virus necessary for maximal expression in 1×10^6 cells 2 d after infection was used in all subsequent infections. Typically, Sf9 cells grown at 27°C in TC100 medium supplemented with 10% heat-inactivated fetal calf serum were harvested 2 d after infection by scraping cells free of the tissue culture dish. After pelleting, cells were either directly solubilized in 2× sample buffer for loading onto gels or were lysed in 1% NP-40/PBS, cleared by centrifugation at 13,000 *g* for 10 min at 4°C and supernatants immunoprecipitated with anti–p127 antibodies.

Immunoelectron Microscopy

Immunoelectron microscopy was performed essentially according to Tokuyasu (1986) and Raska et al. (1990). Shortly, dissected tissue was fixed in aldehyde, either 8% paraformaldehyde or a mixture of 0.1% glutaraldehyde and 4% paraformaldehyde, for 2 h at room temperature. The fixed samples were infused with 2.1 M sucrose in PBS at room temperature, frozen in liquid nitrogen, and cut with tungsten-coated glass knives using a Reichert Ultracut with an FC4 cryoattachment unit. After thawing, the sections were collected on formvar-coated hexagonal grids, blocked with 10% fetal calf serum in PBS, and then incubated with p127 anti–peptide primary antibodies diluted in 5% fetal calf serum in PBS followed by goat anti–rabbit IgG coupled to 10 or 15 nm gold particles (Amersham Corp.). The labeled sections were postembedded in a mixture of methylcellulose and uranyl acetate and inspected in a Philips 300 electron microscope.

Results

Spatio-temporal Expression of p127

The pattern of p127 expression was investigated during *Dro-*

sophila development using immunofluorescence techniques and confocal laser microscopy. As probes for p127 identification, we used two different affinity purified polyclonal antibodies raised in rabbits and directed against two synthetic peptides. These peptides correspond to either the amino terminus (N-38) or the carboxyl terminus (C-39) of the conceptual translation product of the *l(2)gl* gene. Both antibody preparations recognized a protein of ~130 kD in size (p127) on Western blots of proteins extracted from either *Drosophila* embryonic, larval and adult tissues, or *Spodoptera frugiperda* Sf9 cells expressing p127 from recombinant baculoviruses (Sf9:p127) and gave rise to similar results in tissue staining experiments. As a control for the specificity of the antibodies in our immunostaining experiments, we incubated dissected imaginal discs with anti-peptide (C-39) antibodies in the presence or absence of C-39 peptide. As shown in Fig. 1 *C*, the addition of the peptide abolished immunostaining, indicating that the signals observed in our experiments were specific for p127. We also performed immunostaining of *l(2)gl* mutant tissues with anti-peptide (C-39) antibodies and detected no staining (Fig. 1 *E*), again showing that the antibodies used for the immunocytochemistry were specific for p127. To further demonstrate the specificity of the antibodies, we probed Western blots of total *Drosophila* embryonic proteins with the antibody preparations used in the immunocytochemical analysis in the presence and absence of immunizing peptide. The presence of excess peptide completely abolished the detection of p127 (Fig. 1 *G*).

Previous analyses have revealed that *l(2)gl* transcription occurs predominantly during two phases of *Drosophila* development, during early embryogenesis and at the larval to pupal transition phase (Mechler et al., 1985; Merz et al., 1989). Furthermore, earlier transplantation experiments (Gloor, 1943) as well as recent genetic mosaic experiments indicated that the expression of the *l(2)gl* gene is critically required during oogenesis, in both the germ line and the soma (Szabad et al., 1991). Thus, we investigated first the distribution of the *l(2)gl* p127 protein in embryonic and larval tissues, as well as in the reproductive organs of the adult fly.

Embryo

Our studies reveal that during the first half of *Drosophila* embryonic development p127 is ubiquitously expressed in all embryonic cells from the syncytial blastoderm stage up to the germ band retraction stage and, thereafter, becomes gradually restricted to the midgut epithelium by the end of embryogenesis. In the early syncytial embryo, p127 expression is detected as soon as the nuclei reach the cortical cytoplasm where p127 is essentially concentrated in the apical periplasm between the nuclei and the egg surface (Fig. 2, *A-C*). At the cellular blastoderm and early gastrulation stage, p127 is strongly expressed in the apical periplasm of all embryonic cells and to a moderate extent, is present along the growing plasma membranes which extended downward from the cell surface and enclosed each nucleus within a long columnar cell (Fig. 2, *D* and *E*). At the boundary of the periplasm where the concentration of p127 is abruptly decreasing, p127 is visibly forming nodules which are positively stained by anti-p127 antibodies (Fig. 2 *B*). From gastrulation up to germ band extension stage, p127 expression

is ubiquitous and relatively uniform, but somewhat more diffuse in all embryonic cells (Fig. 2, *F* and *G*). During germ band retraction, expression of p127 is diffuse in the cytoplasm as well as localized along the plasma membranes (Fig. 2, *H* and *I*). Thereafter p127 staining becomes more localized to plasma membranes of epithelial cells, such as the midgut cells. The expression in the digestive tract is then maintained during all the larval development up to the mid third larval instar at which time p127 becomes intensively expressed in several other tissues.

Third Instar Larva

Expression of p127 in third instar larvae is particularly strong in all imaginal discs as shown in Fig. 3 (*A-C*), as well as in the proventriculus and midgut epithelium (not shown), and is weaker but still detectable in the salivary glands (Fig. 3 *D*). By contrast to the relatively high level of p127 expression in the imaginal discs, p127 is not detected in the optic centers of the brain hemispheres (Fig. 3 *A*). To control whether the lack of staining in the brain was due to technical reasons such as inadequate fixation or poor antibody accessibility, we dissected brains and imaginal discs of late third instar larvae and analyzed p127 by immunoprecipitation and Western blotting procedures. In no case were we able to detect p127 in brain extracts although we could easily identify p127 in protein extracts from imaginal discs (data not shown). These results strengthen the immunofluorescence data and indicate that despite the high rate of cell proliferation in the optic centers of the brain hemispheres, p127 expression is not required in this tissue during development of the third larval instar.

Imago

In the adult fly, p127 expression occurs predominantly in two different organs: the digestive tract (Fig. 3 *E*) and the reproductive organs (Figs. 3, *F-H*, and 4). From the formation of the digestive tract during embryogenesis at the time of the dorsal closure, we observed a constitutive expression of p127 in the palisadic cells forming the embryonic, larval and adult midgut, as well as in the epithelial cells of the larval and adult proventriculus (Fig. 3 *E*). In addition we found that other epithelial tissues such as the salivary glands are also stained (Fig. 3 *D*), albeit weakly, with anti-p127 antibodies, but we were unable to detect any staining in the Malphigian tubules, the hindgut, the fat bodies, the muscles, and the nervous system. In adult flies, the most intensively p127 expressing tissues were found to be, in females, the ovaries (Fig. 4, *C-H*) and, in males, the apex of the testes (Fig. 4, *A* and *B*) and the epithelial tissues forming the ejaculatory bulb and the accessory glands (Fig. 3, *F-H*).

In the ovaries, p127 is strongly expressed in the germarium and in previtellogenic egg chambers (stages 1-7) and more moderately in vitellogenic egg chambers (Fig. 4, *C-H*). In the germarium p127 displays a heterogeneous pattern of staining that may reflect the composite structure of the germarium made of germ line cells forming clusters of up to 16 interconnected cystocytes engulfed by migrating mesodermal cells detached from the *tunica propria* (Fig. 4 *D*). We interpret the apparently more intense p127 staining as orig-
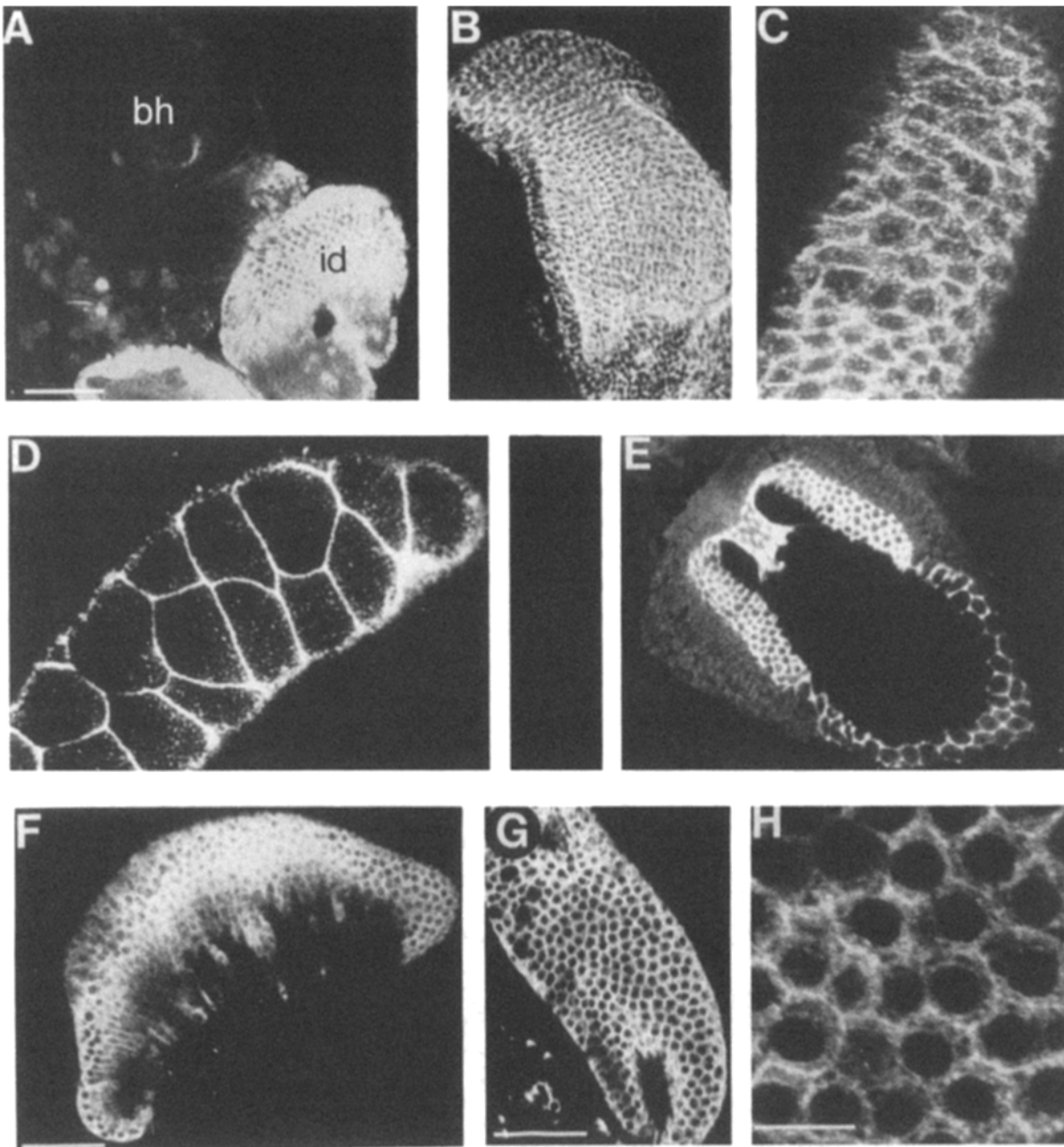
Figure 3. Distribution of p127 in late third instar larvae and in adult digestive tract and male reproductive organs. Confocal microscope images (except *E* which is a thin cryo-section) of dissected, wild-type third instar larva (*A–D*) and adult (*E–H*) tissues, fixed and stained with anti–p127 affinity purified antibodies. (*A*) Optic lobe and eye-antenna disc displaying an intense staining in imaginal discs (*id*) and absence of staining in brain hemispheres (*bh*). (*B* and *C*) Glancing optical sections of eye (*B*) and wing (*C*) imaginal discs illustrating staining at cell boundaries. Note granular and punctate staining in *C*. (*D*) Staining in salivary gland. The signal strength appears intense due to digital processing used to increase the brightness. (*E*) Adult proventriculus showing intense staining at cell to cell contacts. (*F*) Staining in adult male ejaculatory bulb, (*G* and *H*) accessory gland. Note granular staining in all cells as shown in higher magnification in panel H. C-39 antibodies were used for all preparations shown in this figure. Bars: (*A, F,* and *G*) 50 μm; (*H*) 10 μm; (*C*) 5 μm.

inating from the mesodermal cells because the follicle cells derived from the mesodermal cells are intensively stained around the 16-cell cysts forming early egg chambers (stages 1–2). In previtellogenic egg chambers (stages 1–7), p127 is uniformly expressed in all nurse cells, oocytes, and follicle cells (Fig. 3, *C* and *E*). Strikingly, in these early stages of oogenesis, p127 is predominantly located in the cytoplasm of the nurse cells and the oocyte and decorates only moder-

ately the plasma membranes separating these cells. By contrast, in follicle cells, p127 appears to be polarized with a strong localization along the lateral sides of the cells and a virtual absence from the basal and apical membranes of these cells. The absence of membrane localization is particularly noticeable in the regions of contact between the follicle cells and the nurse cells or the oocyte (Fig. 4, *E–H*).

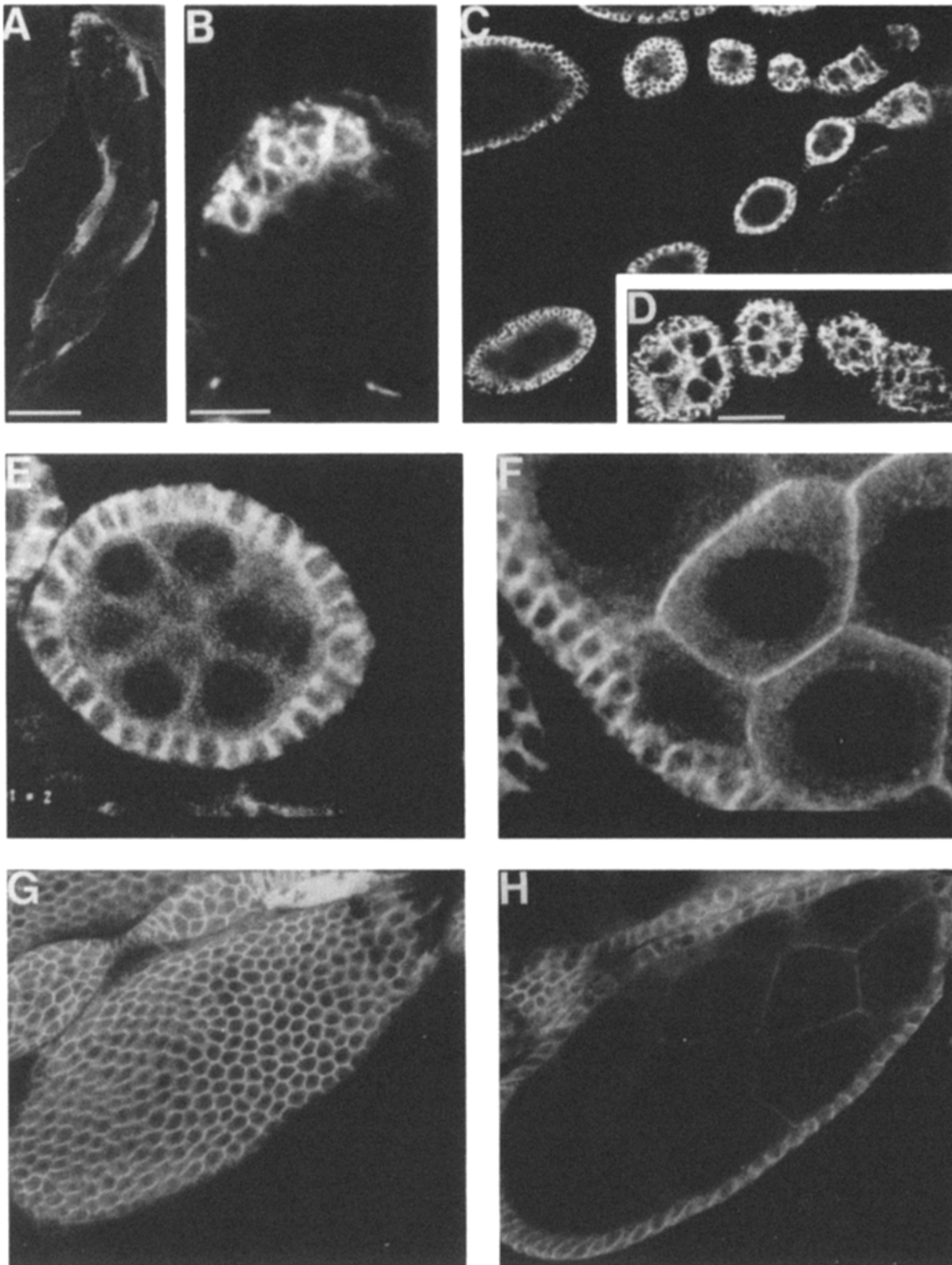In the last previtellogenic stage (stage 7) (Fig. 4 *E*), the

Figure 4. Expression of p127 in adult testis and ovaries. Confocal microscope images of dissected, wild-type adult tissues, fixed, and stained with anti–p127 affinity purified antibodies. (*A*) Overview of testis, and (*B*), a higher magnification of the proximal tip of the same testis. Note staining at the very tip in region of the gonial cells and further down the sperm tube to what is possibly bundles of spermatids. (*C* and *D*) Early egg chambers and germarium. All cells are stained, however the pattern is heterogenous and granular, especially in the germarium and stage 1 and 2 egg chambers. (*E*) Stage 7 egg chamber. (*F*) Stage 9 egg chamber. Staining on lateral membranes and in the cytoplasm of the nurse cells is visible. (*G* and *H*) Lower magnification of stage 9 egg chamber optical sectioned close to the surface, *G*, and through approximately the middle, *H*. Note intense staining at lateral follicle cell boundaries and absence on basal and apical surfaces (also seen in *F*). C-39 antibodies were used for all preparations shown in this figure. Bars: (*A*) 50 μm; (*D*) 25 μm; (*B*) 10 μm.
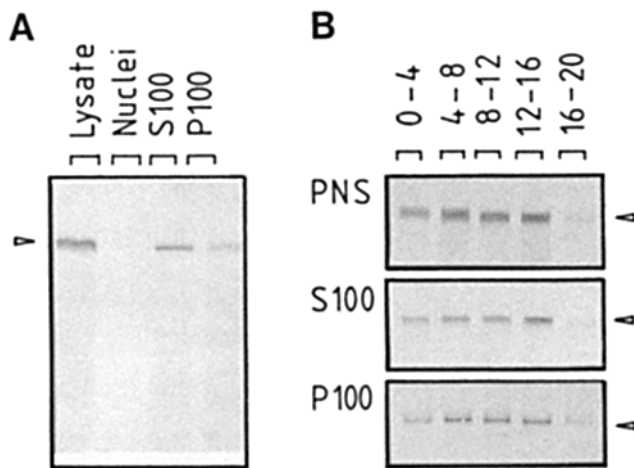
Figure 5. Subcellular distribution of p127. (*A*) Extracts of wild type embryos (*Lysate*) were fractionated into soluble (*S100*), membrane (*P100*), and nuclear components (*Nuclei*). Proteins were separated by 7% SDS/PAGE and analyzed on Western blots using anti–p127 antibodies. (*B*) Lysates from staged (as indicated above figure in hours of development after egg laying at 25°C) wild-type embryos were prepared, centrifuged at low-speed to remove nuclei (post nuclear supernatant, *PNS*), and then separated at 100,000 *g* into soluble (*S-100*) and membrane (*P-100*) fractions. Open arrow heads indicate position of p127. C-39 antibodies were used in *A* and pEX215 antibodies in *B*.

egg chamber begins to elongate and the follicle cells become enlarged and columnar, particularly in the region apposed to the oocyte, and their nuclei polyploidized. As soon as yolk formation begins at stage 8, p127 staining disappears completely from the oocyte and fades gradually in the nurse cells where it becomes undetectable from stage 10. However, during all these stages, the expression of p127 remains intense and uniform in the follicle cells until they become thinner and squamous at stage 11. Then, the follicular epithelium ceases to express p127 with the exception of the anterior located cells which become involved in the formation of the micropyle, the conical chorion structure with a central hole serving as sperm entry point.

In the testis, p127 is predominantly detected at the extreme apex of the sperm tube in a region where the gonial cells, the spermatogonia and the spermatocytes are located (Miller, 1950) (Fig. 4, *A* and *B*). Further down the sperm tube, p127 concentration decreases gradually and seems to be associated with the body of elongated spermatids as indicated by the diffusely twisted p127 staining (Fig. 4 *A*). However, in the abdomen of male flies, the strongest p127 staining is observed in the accessory glands and the ejaculatory bulb, which is constituted of filamentous tubules attached to a bulb of epithelial cells (Fig. 3, *F* and *G*). As shown in Fig. 3 *H*, antibody staining reveals a granular distribution of p127 protein in the cytoplasm and a discontinuous pattern of dots along the plasma membrane of the cells of the accessory gland.

Subcellular Distribution of p127

To estimate the relative importance of the cytoplasmic versus membrane-associated form of p127, we have fractionated a postnuclear supernatant fraction of *Drosophila* embryonic

extracts into a membrane-containing cell organelle fraction (P100) and a soluble fraction (S100) by high-speed centrifugation (100,000 *g*). Western blot analyses of total cellular extracts and individual fractions derived from an equal number of embryos were performed. As shown in Fig. 5 *A*, p127 can be found in both membrane and cytosolic fractions but cannot be detected in the nuclear fraction. Furthermore, upon fractionation of the P100 material on a discontinuous sucrose density gradient, p127 is recovered in a fraction that by electron microscopic examination appears essentially made of smooth membrane vesicles, presumably derived from the plasma membrane (data not shown), showing that p127 is directly associated with membrane. Examination of p127 distribution during embryogenesis reveals that, at all embryonic stages so far examined, both a cytosolic and a membrane-associated form can be observed (Fig. 5 *B*). Furthermore, during later embryonic stages the proportion of p127 in the membrane fraction increases. However, this relative increase of p127 in the membrane fraction is accompanied by a strong decrease of the total amount of p127 suggesting that there may be a limited number of binding sites on the plasma membrane with the excess of p127 remaining in the cytoplasm.

p127 Protein Binds to the Inner Face of the Plasma Membrane

Our cell staining experiments and cell fractionation studies showed that an appreciable proportion of p127 can be associated with the plasma membrane. However, these studies have not revealed the orientation of p127 with respect to the plasma membrane insofar as whether any portion of p127 can cross the plasma membrane and be exposed on the cell surface or whether p127 is an intracellular peripheral membrane protein. To address this question we have analyzed the topology of p127 with regards to the plasma membrane in both primary *Drosophila* embryonic cells of Sf9:p127 cells using three different approaches: (*a*) sensitivity to proteases, (*b*) accessibility to antibody staining in intact and detergent-permeabilized cells, and (*c*) cell surface protein labeling.

The sensitivity of p127 to proteolytic cleavage by trypsin was determined in intact primary *Drosophila* embryonic cells and extracts of these cells. As shown in Fig. 6 *A*, p127 present in intact embryonic cells was insensitive to proteolytic digestion by trypsin. In contrast, when these cells were treated with mild detergents such as 1% Triton X-100, p127 became completely sensitive to trypsin digestion. Furthermore, we can show that the disappearance of p127 in the detergent extracts was not due to non-specific degradation of p127 because we were able to prevent proteolytic digestion by adding trypsin inhibitor. We observed no change in our results when 5 mM EGTA was included in the digestion buffer, showing that the resistance of p127 to trypsin digestion in intact cells is not Ca^{2+} dependent (data not shown). These results indicate that no domain of p127 is exposed on the surface of *Drosophila* embryonic cells.

Accessibility of p127 to antibody staining was determined in both intact and saponin-permeabilized Sf9:p127 cells incubated with anti–p127 antibodies. As can be seen in Fig. 6 *B*, only those cells treated with saponin could be stained with anti–p127 antibodies raised against the amino or carboxyl ends, or against the central domain of p127. The requirement
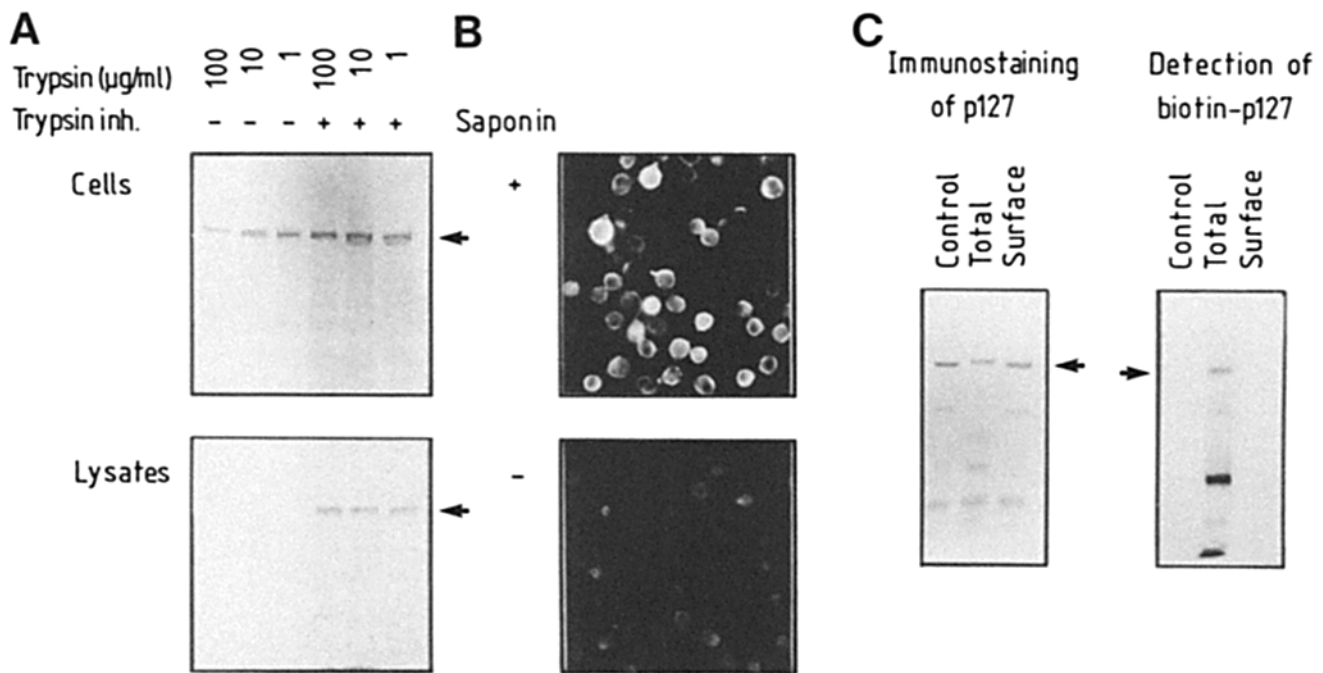
A

Trypsin (µg/ml) 100 10 1 100 10 1 **B**

Trypsin inh. − − − + + + Saponin

Cells

+

←

Lysates

−

←

C

Immunostaining of p127 Detection of biotin-p127

Control Total Surface Control Total Surface

← →

Figure 6. Analysis of the membrane topology of p127. (*A*) Sensitivity of p127 to proteolytic cleavage by trypsin. Intact embryonic cells were incubated with the indicated amount of trypsin for 15 min in the absence (*top*) or presence (*bottom*) of 1% Triton X-100. As a control for the specificity of the trypsin digestion, trypsin inhibitor was added to 200 µg/ml in parallel samples. After digestion, samples were analyzed by Western blotting with anti–p127 antibodies. (*B*) Fixed Sf9:p127 cells were permeabilized with 0.1% saponin (*top*) to allow access to internal epitopes or probed intact (*bottom*) for surface epitopes with antibodies against p127. To visualize bound antibodies, cells were incubated with goat anti–rabbit antibodies conjugated to Texas red. (*C*) Sf9:p127 cells were surface labeled with an activated biotin derivative, NHS-LC-biotin, lysed with detergent, and p127 immunoprecipitated with anti–p127 antibodies (*Surface*). To check for the reactivity of the NHS-LC-biotin to p127, detergent lysates of Sf9:p127 cells were reacted with NHS-LC-biotin and p127 immunoprecipitated (*Total*). As control for the specificity of the avidin-gold reagent, Sf9:p127 cells were processed in parallel as above, without exposure to the NHS-LC-biotin (*Control*). Half of each of the immunoprecipitates were loaded onto two PAGE gels. After Western blotting, one blot was probed with anti–p127 antibodies (*left*) and the other with avidin–gold conjugate to detect biotin (*right*). The additional protein bands detected on the immunoblots are due to a non-specific cross reaction with the C-39 antibody preparation used in this experiment. The two strong biotinylated proteins of lower molecular weight indicated by asterisks may represent binding partners co-immunoprecipitating with p127. The arrows in *A* and *C* mark the position of p127. pEX215 antibodies were used in *A*, C-39 in *B* and *C*.

of a saponin treatment for positively staining Sf9:p127 cells further shows that the p127 protein is entirely located within the cell.

In an additional series of experiments, we have tested whether p127 can be labelled on the surface of cells by using an activated biotin derivative, NHS-LC-biotin (Fig. 6 *C*). Intact Sf9:p127 cells or detergent lysed extracts of these cells were incubated with NHS-LC-biotin. After termination of the reaction, the intact cells were lysed with detergent and p127 was immunoprecipitated from both cell extracts. In addition an immunoprecipitation of an extract that was not exposed to NHS-LC-biotin was included as a control. Half of each immunoprecipitate was identically loaded on two polyacrylamide gels, the proteins separated by electrophoresis and Western blotted. Subsequently, one blot was probed for p127 using anti–p127 antibodies and the other blot was tested for biotinylation using an avidin–gold reagent and silver enhancement. Fig. 6 *C* shows that, although p127 is present in each cell extract, it has only been biotinylated in the cells which have been detergent-treated prior to the addition of the NHS-LC-biotin reagent. This experiment demonstrates again that no part of the p127 protein can cross the plasma membrane and be exposed at the surface of cells.

Immunoelectron Microscopy

To determine more accurately the region or junctional specializations to which p127 is associated on the plasma membrane, we have used immunoelectron microscopic techniques of ultrathin cryosections. For performing this analysis we have chosen the proventriculus of third instar larvae because in this tissue p127 can only be detected in the vicinity of the plasma membranes facing contiguous cells similar to what can be observed in the adult proventriculus (see Fig. 3 *E*). Moreover, p127 appears to be intensively and uniformly distributed along the entire length of the lateral plasma membranes and absent from the basal and apical cell membranes as well as from any region of the cytoplasm.

Immunoelectron microscopic examination of the proventriculus epithelial cells revealed that, p127 is associated with junctional specializations that resemble smooth septate junctions (Noirot-Timothee and Noirot, 1980; Fawcett, 1981; Tepass and Hartenstein, 1994). In the proventriculus, the smooth septate junctions start close to the gut lumen around the apex of the cell extending basally and are characterized by a 17 to 18 nm space between adjacent cells that is filled with a uniformly dense staining material.
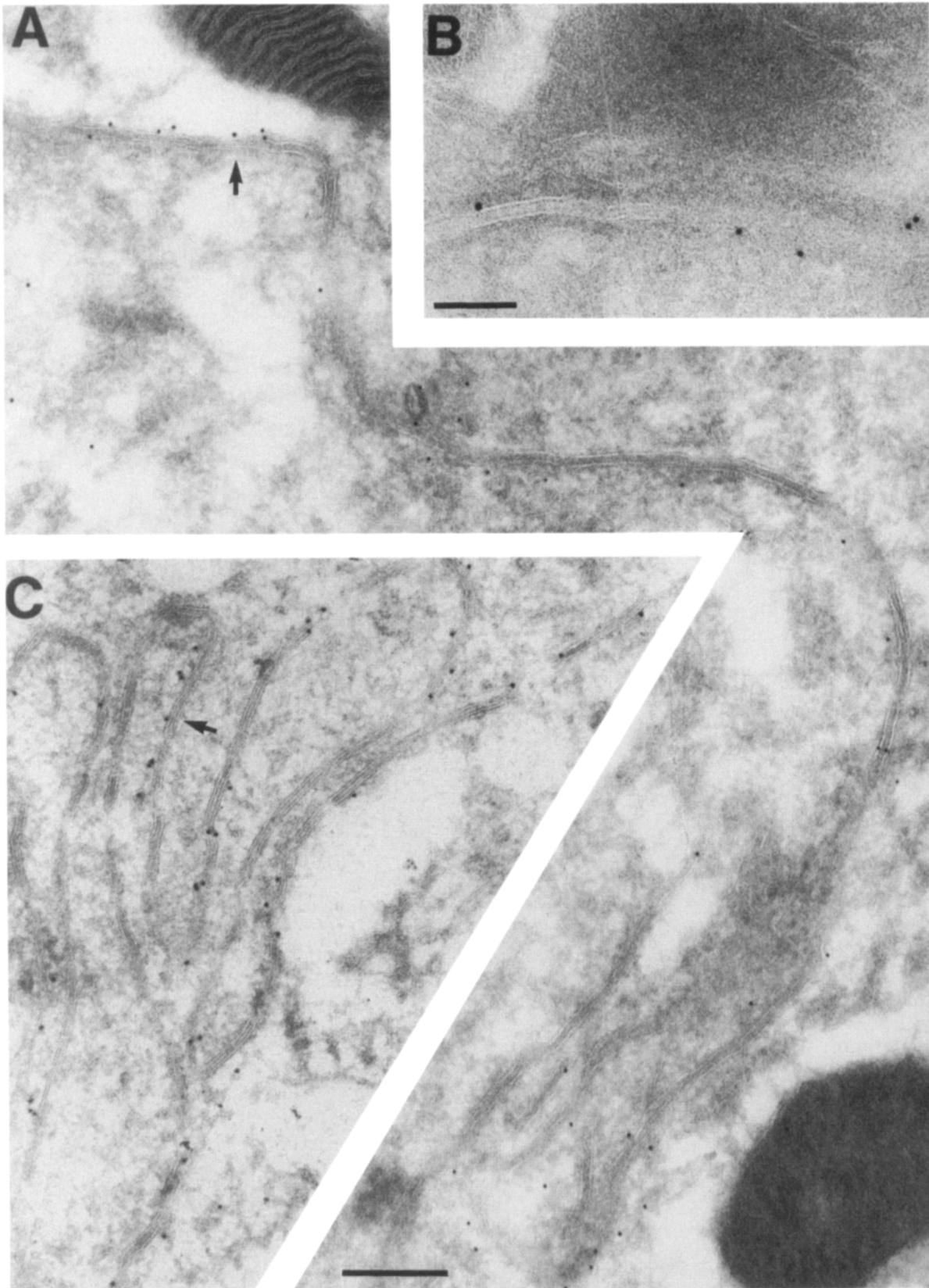
Figure 7. Immunoelectron microscopic labeling for p127 in ultrathin cryosections of third instar larva proventriculus. (*A* and *C*) Smooth septate junctions indicated by arrowheads. (*B*) Higher magnification of smooth septate junction. Gold particles lie primarily along lateral cell membranes and seldom in the cytoplasm. C-39 antibody preparation was used. Bars: (*A* and *C*) 200 nm; (*B*) 100 nm.
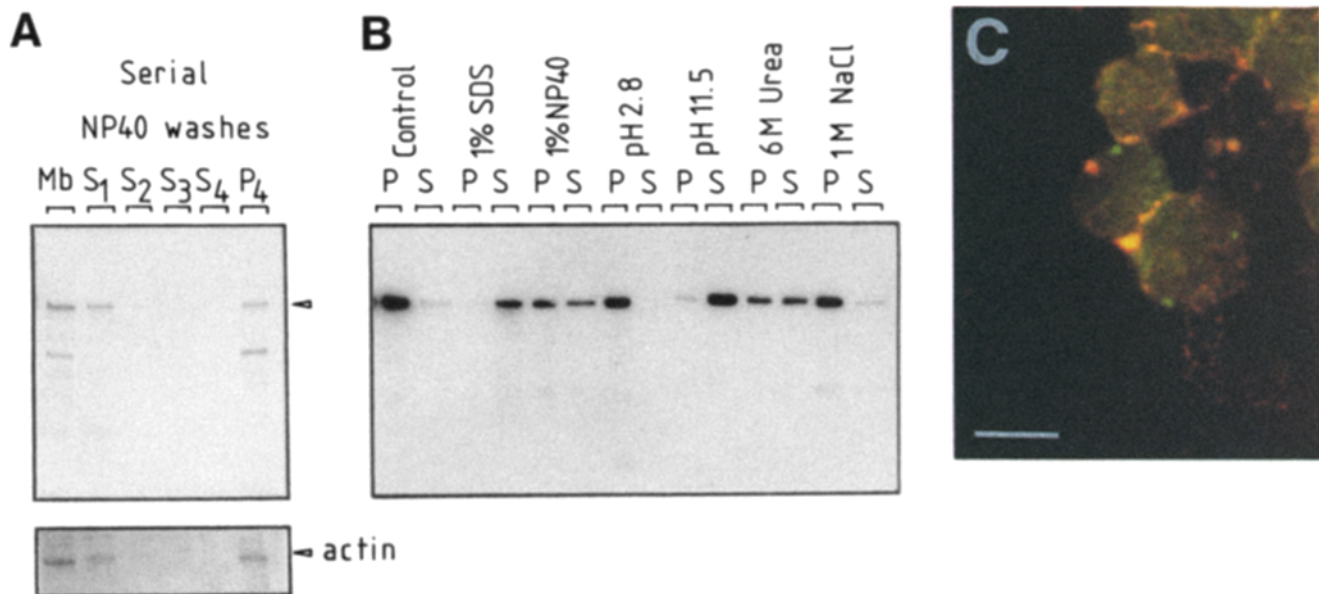
Figure 8. A fraction of the membrane-associated p127 is resistant to solubilization by non-ionic detergents. A membrane fraction was prepared by flotation in a sucrose density gradient from wild-type embryos and treated with repeated washes of NP-40 (*A*) or with various solubilizing reagents (*B*). (*A*) The membrane fraction (Mb) was treated with 1% NP-40, the insoluble material recovered by centrifugation, and washed again through four cycles of 1% NP-40. The supernatants from each wash (S_1–S_4) and the last pellet (P_4) were analyzed by SDS-PAGE and Western blotting. Upper panel is probed with anti–p127 antibody and the lower panel with anti-actin antibody. The additional band detected on the blot is due to a non-specific cross reaction with the C-39 antibody preparation used in this experiment. (*B*) The membrane fraction was treated with PBS (*Control*) or with reagents as indicated above the panel for 30 min at room temperature before separation by centrifugation into pellet (*P*) and supernatant (*S*) fractions. The proteins were separated by SDS-PAGE and analyzed by Western blotting using anti–p127 antibodies. The pellet contains the insoluble fraction whereas the supernatant corresponds to the soluble fraction. (*C*) Sf9:p127 cells grown on glass cover slips were extracted with 0.2% NP-40 before fixation and double labeled with anti–p127 antibodies and goat anti-rabbit Texas red to visualize p127 and phalloidin coupled to FITC to visualize F-actin. Confocal laser scan images were collected on separate channels simultaneously and processed to show p127 as red and actin as green. The yellow color represents coincidental staining and is localized primarily to the region of cell to cell contacts. C-39 antibodies were used for all experiments shown in this figure. Bar, 10 μm.

As shown in Fig. 7 the gold particles bound to p127 are associated with junctional domains of the lateral plasma membrane corresponding to smooth septate junctions. This pattern is typical for what we observed in the various specimens that were immunolabeled by means of gold adducts. Whether we used antibodies recognizing the amino or carboxyl ends of p127, we found that the gold particles were uniformly scattered along the plasma membranes on the lateral sides of the cell. No labeling can be identified on the apical or basal plasma membranes and few gold particles were found in the cytoplasm. The majority of the gold particles are located on the inner face of the plasma membranes and few particles are laying over the membranes. The immunoelectron microscopic data further indicate that p127 is located within the cell and can be intimately associated with the inner side of plasma membrane along junctional domains.

p127 Interaction with the Plasma Membrane

Since a significant proportion of p127 can be recovered in a membrane cell organelle containing fraction, we have analyzed the nature of p127 association with membranes. The amino acid sequence of p127 does not reveal any transmembrane or secretory signal peptide sequences (Jacob et al., 1987; Gateff and Mechler, 1989; Hortsch and Goodman, 1991). We have biochemically investigated whether p127 may carry any posttranslational modifications that may con-

fer membrane anchoring properties such as addition of glycosylphosphatidyl inositol (GPI)-anchors or acylation with fatty acids and found no obvious modifications in p127 (results not shown).

A number of proteins have been shown to be localized to the plasma membrane by interaction with the cortical cytoskeleton (Bretscher, 1991). We have examined the membrane association of p127 by using selective detergent extraction procedures and solubilizing agents which have been previously used to study interactions of proteins with the cytoskeleton (Geiger, 1983; Graziani et al., 1989; Nagafuchi and Takeichi, 1988; McCrea and Gumbiner, 1991). When a membrane fraction purified by flotation in a sucrose density gradient is treated with a non-ionic detergent such as NP-40, a large proportion (~50–75%) of the membrane associated p127 was recovered as large insoluble aggregates. Repeated detergent washes of the insoluble membrane material did not result in further release of p127, indicating that the insoluble p127 is participating in large quaternary structures. Furthermore, as shown in Fig. 8 *A*, the insoluble fraction also contains actin, showing that p127 co-sediments with elements of the membrane skeleton. In addition, treatments with various solubilizing agents such as 6 M urea released about the same proportion of p127 from the membrane fraction as the non-ionic detergent treatment, leaving the majority of p127 in an insoluble form, whereas high salt (1 M NaCl) and low pH were less effective in solubilizing p127. By contrast, the use of strong ionic detergents such as

1% sodium dodecylsulfate or high pH solubilized p127 effectively (Fig. 8 B).

Furthermore, double immunostaining of non-ionic detergent-treated Sf9:p127 cells revealed that the majority of the detergent-insoluble p127 is colocalized with the actin based cytoskeleton in cortical domains adjacent to contiguous cells (Fig. 8 C). Thus, by applying procedures that have been used to analyze membrane cytoskeletal proteins, we can show that p127 displays similar characteristics. All together these results with those of the confocal and electron microscopy suggest strongly that the binding of p127 to the membrane domains of contact between adjacent cells is mediated by elements of the cytoskeletal matrix undercoating the plasma membrane.

Discussion

Our studies reveal that the *l(2)gl* gene is expressed in a large variety of tissues throughout development from the onset of blastoderm formation up to adulthood and shed light on *l(2)gl* function which previously was essentially inferred from phenotypic analysis or gauged by marginal homologies to other proteins. Our analyses show that *l(2)gl* encodes an intracellular protein displaying characteristics of a cytoskeletal protein which may directly contribute to the structure and maintenance of cellular architecture, and thus to tissue organization. The structural alterations induced by *l(2)gl* inactivation may, in turn, reduce the potential of a cell to receive and process inter- and intracellular signals, and can be therefore critical for differentiation. By blocking or altering the reception of signals, these disruptions prevent the cells from progressing in their normal program of development and keep them as undifferentiated stem cells which continue to grow and divide.

In this paper, we have presented data regarding the spatio-temporal expression of the *l(2)gl* encoded protein p127, its intracellular distribution and its involvement in a cytoskeletal network undercoating the plasma membrane and extending into the cytoplasm. The broad distribution of p127 in *Drosophila* development includes: (*a*) an ubiquitous but transient expression during early embryogenesis, (*b*) a uniform and apparently constitutive expression in the midgut epithelium of the larval and adult digestive tract and proventriculus, (*c*) a spatially and temporally regulated expression in several larval and imaginal organs, and (*d*) a strong expression in both female and male gonads as well as in the accessory organs of the male genital tract.

p127 Expression in Ovaries and Testes

Previous studies involving ovary transplantation into normal third instar larvae (Hadorn and Gloor, 1942; Gloor, 1943; for review see Hadorn, 1961) have revealed that the implanted *l(2)gl* ovaries develop synchronously with the metamorphosing host and, at the time of hatching, apparently reach the same stage as normal ovaries. However, the development of the egg chambers is profoundly perturbed with variable number of nurse cells and an incomplete layer of follicle cells grouped together in a disorganized mass resembling tumors (Gloor, 1943). In addition, recent analyses involving pole cell transplantation and genetic mosaics have shown that the absence of *l(2)gl* function in either the germ

line or the follicle cells prevents egg development (Szabad et al., 1991). Our immunofluorescence studies demonstrate that in the adult female ovary both types of proliferating cells (the germ line as well as the mesodermally derived follicle cells) express high level of p127. This intense p127 expression presumably begins during the early larval stages of ovary development (i.e., in the dividing stem cell oogonia) as suggested by the β-galactosidase staining found in ovaries of second and third instar larvae containing an *l(2)gl-lacZ* transgenic reporter gene (data not shown), and is also most visible in the germarium and in previtollogenic egg chambers in adult ovaries. These observations support the notion that *l(2)gl* involvement in cytoskeletal organization is required for the differentiation of the egg chambers and is necessary in both germ line and follicle cells.

The *l(2)gl* function also contributes to the differentiation of the male germ line and is already required at the end of embryogenesis as shown by the degeneration of the male gonads in hatching *l(2)gl*-deficient larvae (Hadorn and Gloor, 1942; Gloor, 1943). By comparison to the female germ line, the earlier requirement of *l(2)gl* in the development of the male germ line may only reflect the more precocious ontogenesis of the testes which begins with the onset of larval life whereas ovary ontogenesis occurs during metamorphosis. Interestingly, we found that in adult testes p127 is essentially expressed in stem cells and early differentiating spermatocytes. Thus, with the knowledge that the male germ line is degenerated in *l(2)gl*-deficient first instar larvae, we favor the hypothesis that p127 may control spermatogonial proliferation and early differentiation of the spermatocytes, and, thus, can be required in a similar fashion in the developing testes during early larval stages.

Embryonic p127 Expression and the Tumorous Phenotype

The absence of p127 expression, as revealed by the lack of both immunostaining and β-galactosidase expression of a *l(2)gl-lacZ* reporter gene (data not shown), in the anlagen of the imaginal discs and in the brain hemispheres during second and early third larval instars, at a time when the first growth abnormalities become visible in the mutant tissues (Hadorn, 1961; Gateff and Schneiderman, 1969; Gateff, 1978), indicates that the critical period of p127 expression for preventing tumorigenesis occurs at a much earlier developmental stage, namely, during embryogenesis when p127 expression is strong and uniform in all embryonic cells. This is the only developmental period during which the primordia of both organs forming tumors in *l(2)gl*-deficient larvae are strongly expressing p127. The importance of embryonic p127 expression in the control of cell growth of the imaginal discs and the brain hemispheres during larval development is further supported by experimental data. Transplantation experiments of tissues from mutant embryos have revealed that the *l(2)gl* embryonic cells are already committed to malignant growth (Gateff and Schneiderman, 1974). Furthermore, gynandromorph experiments have shown that brain and imaginal discs tumors can only occur in *l(2)gl*-deficient clones produced before blastoderm formation (Merz et al., 1989), whereas clones formed during larval development differentiate normally (Cline, 1976).

Our immunocytochemical data confirm therefore that the

critical period for the establishment of tumorigenesis occurs in embryonic cells and further indicate that the third instar larval expression of p127 in the imaginal discs bears no direct contribution to the control of cell proliferation in this tissues. The irrelevance of the late larval p127 expression with regards to the control of imaginal disc growth is further supported by the finding that p127 is not expressed in brain hemispheres of normal third instar larvae or is only synthesized in such a reduced amount that it cannot be detected by immunocytochemistry or immunoblotting techniques of dissected brains. Furthermore, the difference in p127 expression between brain and imaginal disc tissues appears to be an intrinsic characteristic of these tissues since a *lacZ* transgenic reporter gene under the control of an *l(2)gl* promoter displays a similar difference of expression in tumorous tissues, as revealed by a strong positive staining for β-galactosidase in imaginal disc tumors and a barely detectable expression of *lacZ* in the malignantly transformed brain hemispheres (data not shown). One interpretation for explaining the absence of p127 in brain and its presence in imaginal discs may be found in the difference of cell structure between these two tissues. The neuroblasts exhibit a spheroidal morphology with no apparent apical–basal orientation whereas the imaginal disc cells are organized in a monolayer epithelial sheet and characterized by a strong apical–basal cell polarity. If p127 is a cytoskeletal component contributing to the organization of the cell structure and more particularly to the establishment and maintenance of cell polarity, we would expect that the expression of p127 is required in imaginal disc cells. Such a requirement would not be necessary in neuroblasts which display a less polarized organization.

Immunocytochemistry also revealed that p127 is expressed in a series of tissues displaying minor phenotypic abnormalities, such as the salivary glands and their imaginal rings. In *l(2)gl*-deficient larvae, the cells of the salivary glands are smaller in size (Grob, 1952) and their chromosomes show a low degree of polytenization (Welch, 1957) whereas the number of cells present in the imaginal rings of the salivary glands is markedly reduced (Grob, 1952). In addition, p127 expression can also occur in tissues exhibiting no obvious phenotypic alterations. This is particularly the case of the midgut epithelium (Grob, 1952) in which p127 is expressed constitutively, in developing as well as in terminally differentiated tissues.

Intracellular Localization of p127

Our immunohistochemical and biochemical investigations show that p127 is an intracellular protein which can be either localized in the cytoplasm, or bound to the internal face of the plasma membrane. These findings are in contrast to previous reports which, on the sole basis of immunocytochemical analysis of embryo sections and marginal alignments of compared protein sequences, have assigned an extracellular location to the *l(2)gl* gene product and predicted properties with two distinct types of cell adhesion molecules (Lützelschwab et al., 1987; Klämbt et al., 1989; Bryant and Schmidt, 1990), although we and others have expressed doubts on such an extracellular assignment (Jacob et al., 1987; Gateff and Mechler, 1989; Merz et al., 1990; Hortsch and Goodman, 1991). To date all characterized cell adhesion

molecules have either intracellular, transmembrane, and extracellular domains, or are attached to the external face of the plasma membrane by glycosyl-phosphatidylinositol anchors. Furthermore, due to posttranslational modifications, such as proteolytic cleavage and glycosylation, the apparent molecular weight of cell adhesion proteins or membrane receptors, as determined by SDS-PAGE electrophoresis, is usually different from the molecular weight predicted from cDNA sequences. As shown by our analyses, all these features are lacking in p127.

In addition, by using three different immunobiochemical procedures, we can show that no part of p127 is exposed on the cell surface. Our findings show that p127 is an intracellular protein.

p127 Is Part of a Cytoskeletal Network Which Extends Into the Cytoplasm and Can Undercoat the Plasma Membrane

The remarkable distribution of p127 that we document in different cell types indicates that p127 forms or participates in a cytoskeletal network. Our cell fractionation studies show that we can find p127 in a cytosolic form and in a form tightly associated with the plasma membrane. The plasma membrane association of p127 may correspond to a bona fide physical binding to elements of the membrane cytoskeleton as revealed by the insolubility of p127 in non-ionic detergents and the presence of actin in these insoluble complexes. Whether p127 binds directly to actin or is bound via another protein(s) remains to be determined. Similarly, in the cytoplasm, p127 appears to participate or to build by itself a cytoskeletal network whose other elements are beginning to be unraveled. In particular, we found that p127 interacts with non-muscle myosin II heavy chain. Furthermore, both on the membrane or in the cytosol, p127 is always recovered in large oligomeric complexes (Strand et al., 1994). Analysis of these complexes has revealed that p127 is the predominant component, suggesting that p127 can by itself form quaternary structures. These data, taken together with the association of p127 in large multi-protein complexes, of which one component is a serine kinase that specifically phosphorylates p127 (data not shown), support a model in which p127 may act by coordinating elements of a cytoskeletal network and by contributing to a signaling pathway regulating cell growth.

The participation of p127 in a cytoskeletal network is further strengthened by the results of our microscopic examination. First of all, the intracellular p127 distribution displays considerable variability according to the cell type and to the period of development. The asymmetric pattern of accumulation of p127 at the apical ends of blastoderm cells is highly reminiscent of the pattern of distribution of cytoskeletal components including actin, spectrin, and non-muscle myosin (Warn and Robert-Nicoud, 1990; Karr and Alberts, 1986; Pesacreta et al., 1989; Young et al., 1991) which has been observed in syncytial blastoderm and cellular blastoderm embryos. Moreover, the distribution of p127 over the somatic nuclei of the blastoderm egg can vary in a similar fashion as non-muscle myosin (Young et al., 1991), forming either a cortical cap or ring (data not shown). The apparent similar subcellular localization of p127 and non-muscle myosin at syncytial blastoderm suggests that p127 plays an active

role during the cellularization process and in cytokinesis, although we have no direct evidence that p127 can exert chemomechanical force. Furthermore, the diffuse and changing pattern during gastrulation and germ band extension and retraction can be linked to a time of development when there is extensive cell movements and modifications in cell structure. In the cytoplasm of the nurse cells and follicle cells and in secretory tissues such as the ejaculatory bulb and accessory glands, we speculate that, in addition to the organization of the membrane cytoskeleton at cell junctions, p127 may be associated with a cytoskeletal network controlling intracellular organelle transport. Another gene, *shibire*, à *Drosophila* homolog to the vertebrate microtubule-associated protein, dynamin (Chen et al., 1991), is apparently playing a role in membrane cycling and intracellular vesicular transport (Poodry and Edgar, 1979; van der Bliek and Meyerowitz, 1991). Interestingly, mutations in *shibire* cause pleiotrophic effects, including muscle paralysis or development abnormalities such as the tumorous overgrowth of embryonic neuroblasts, suggesting that structural disruptions in microtubule functions can have effects not only on cell fate choices but also on the regulation of cell proliferation, in a very similar way as to what can be seen in *l(2)gl* mutations (Poodry, 1990).

With the exception of the male germ line, cell death is not a major effect of *l(2)gl* inactivation. In the other tissues, the absence of p127 is either imperceptible or barely perceptible and it becomes only detectable when defined cells resume their proliferation during larval development. In the imaginal disc cells and the neuroblasts of the optic lobes, the absence of p127 induces changes which render cells unable to recognize their environment and result in unrestricted growth. We would argue that these changes are caused by subtle modifications of the cytoskeletal architecture with two direct consequences: loss of cell polarity and disruption of intercellular communication directing cell differentiation. Although *l(2)gl* is intensively expressed during embryogenesis, its inactivation does not impair morphogenesis but profoundly alters organogenesis by preventing terminal cell differentiation to occur in tissues, such as the imaginal disc primordia, the optic lobes in the brain and the ovaries.

There is growing evidence that a number of proteins may fulfill similar roles in coordinating cytoskeletal-based inter- and intracellular communication during development (Peifer et al., 1993; Trofatter et al., 1993; Rouleau et al., 1993; Tsukita et al., 1991; Woods and Bryant, 1991; Volberg et al., 1992; Su et al, 1993; Rubinfeld et al., 1993; Wiegant et al., 1986). In particular, genetic and phenotypic analyses of the *Drosophila armadillo* gene, a homolog to the vertebrate β-catenin and plakoglobin genes (McCrea et al., 1991), suggest that the *armadillo* protein not only plays a critical role in the intercellular *wingless* signaling pathway but can be also a component of cell adherens junctions, and therefore may contribute to the integrity and maintenance of the actin-based cytoskeleton (Peifer, 1993). However, mutations in *armadillo* lead to much more severe defects than the ones caused by *l(2)gl* resulting in embryonic cell death and not causing cell proliferation. Thus *armadillo* is likely to be involved in a different process than the one controlled by *l(2)gl*. In a case more similar to *l(2)gl*, the inactivation of the *Drosophila lethal(l)discs large-1 (dlg-1)* gene leads to overgrowth of imaginal discs. The proposed *dlg-1* gene product

displays regions of homology not only to guanylate kinases (Bryant and Woods, 1992) but also to a submembrane plaque protein, ZO-1 (Tsukita et al., 1993). Moreover, recent analysis suggests that a candidate neurofibromatosis two tumor suppressor protein designated as "merlin" or "schwannomin," is closely related to proteins proposed to link cytoskeletal components with the membrane (Trofatter et al., 1993; Rouleau et al., 1993). A defect in merlin/schwannomin may disrupt some aspect of the plasma membrane cytoskeleton and displays similarities with the defects caused by *l(2)gl*.

Our immunoelectron microscopy data suggest that p127 is more a component of a general membrane undercoating matrix rather than a structural component of a specific type of cellular junctions. This interpretation is further supported by the finding that cellular junctions can be found in *l(2)gl* tumorous imaginal discs, albeit in a reduced number or decreased surface area (Ryese and Nagel, 1984; data not shown).

Our cell biological and biochemical studies complement earlier studies that have demonstrated the importance of *l(2)gl* function in processes such as cell differentiation and organogenesis by showing the precise subcellular localization of the *l(2)gl* gene product, p127, and its interaction with defined domains of the plasma membranes. Further experiments should allow us to directly isolate proteins that are associated with p127 and eventually study the interactions of these proteins both biochemically and genetically. Such information may provide further insights into the mechanisms controlling cell growth and differentiation.

References

Ashburner, M. 1989. *Drosophila*: A Laboratory Manual. Cold Spring Harbor Laboratory Press, Cold Spring Harbor, NY. 1–434.
Aggarwal, S. K., and R. C. King. 1969. Comparative study of the ring glands from wild-type and *l(2)gl* mutant *Drosophila melanogaster. J. Morphol.* 129:171–199.
Bretscher, A. 1991. Microfilament structure and function in the cortical cytoskeleton. *Annu. Rev. Cell Biol.* 7:337–374.
Bryant, P. J., and O. Schmidt. 1990. The genetic control of cell proliferation in *Drosophila* imaginal discs. *J. Cell Sci.* 97(Suppl.)13:169–189.
Bryant, P. J., and D. F. Woods. 1992. A major palmitoylated membrane protein of human erythrocytes shows homology to yeast guanylate kinase and to the product of a *Drosophila* tumour suppressor gene. *Cell.* 68:621–622.
Chen, M. S., R. A. Obar, C. C. Schroeder, T. W. Austin, C. A. Poodry, S. C. Wadsworth, and R. B. Vallee. 1991. Multiple forms of dynamin are encoded by *shibire*, a *Drosophila* gene involved in endocytosis. *Nature (Lond.).* 351:583–586.

Cho, K.-O., C. A. Hunt, and M. B. Kennedy. 1992. The rat brain postsynaptic density fraction contains a homolog of the *Drosophila* discs-large tumor suppressor protein. *Neuron.* 9:929–942.

Cline, T. 1976. Rescue of a neoplastic mutant. *Genetics.* 83:16s.

Fawcett, D. W. 1981. *The Cell.* W. B. Saunders Company, Philadelphia. 1–862.

Gateff, E. 1978. Malignant neoplasms of genetic origin in *Drosophila melanogaster. Science (Wash. DC).* 200:1448–1459.

Gateff, E., and B. M. Mechler. 1989. Tumour suppressor genes of *Drosophila melanogaster. CRC Crit. Rev. Oncogenesis.* 1:221–245.

Gateff, E., and H. A. Schneiderman. 1969. Neoplasms in mutant and cultured wild-type tissues of *Drosophila. Natl. Cancer Inst. Monogr.* 31:365–397.

Gateff, E., and H. A. Schneiderman. 1974. Developmental capacities of benign and malignant neoplasms of *Drosophila. Wilhelm Roux Arch. Entwicklungsmech. Org.* 176:23–65.

Geiger, B. 1983. Membrane-cytoskeleton interaction. *Biochem. Biophys. Acta.* 737:305–341.

Gloor, H. 1943. Entwicklungsphysiologische Untersuchung an den Gonaden einer Letalrasse (*lgl*) von *Drosophila melanogaster. Rev. Suisse Zool.* 50:339–394.

Graziani, G., R. Ron, A. Eva, and S. Srivasta. 1989. The human *dbl*-protooncogene product is a cytoplasmic phosphoprotein which is associated with the cytoskeletal matrix. *Oncogene.* 4:823–829.

Grob, H. 1952, Entwicklungsphysiologische Untersuchungen an den Speicheldrüsen, dem Darmtrakt und den Imaginalscheiben einer Letalrasse (*lgl*) von *Drosophila melanogaster. Z. Vererbungsl.* 84:320–360.

Hadorn, E. 1937. An accelerating effect of normal "ring glands" on puparium formation in lethal larvae of *Drosophila melanogaster. Proc. Natl. Acad. Sci. USA.* 23:478–484.

Hadorn, E. 1938. Die Degeneration der Imaginalscheiben bei letalen *Drosophila*-Larven der Mutation *Lethal-giant. Rev. Suisse Zool.* 45:425–429.

Hadorn, E. 1961. Developmental Genetics and Lethal Factors. Methuen and Co. Ltd., London. 1–355.

Hadorn, E., and H. Gloor. 1942. Die Auswirkung eines Letalfaktors (*lgl*) bei *Drosophila melanogaster* aus Wachstum und Differenzierung der Gonaden. *Rev. Suisse Zool.* 49:228–236.

Harlow, E., and D. Lane. 1988. *Antibodies: A Laboratory Manual.* Cold Spring Harbor Laboratory Press, Cold Spring Harbor, NY. 1–726.

Hortsch, M., and C. S. Goodman, 1991. Cell and substrate adhesion molecules in *Drosophila. Annu. Rev. Cell Biol.* 7:505–557.

Jacob, L., M. Opper, B. Metzroth, B. Phannavong, and B. M. Mechler. 1987. Structure of the *l(2)gl* gene of *Drosophila* and delimitation of its tumour suppressor domain. *Cell.* 50:215–225.

Karr, T. L., and B. M. Alberts. 1986. Organization of the cytoskeleton in early *Drosophila* embryos. *J. Cell Biol.* 103:1494–1509.

Klämbt, C., S. Müller, R. Lützelschwab, R. Rossa, F. Totzke, and O. Schmidt. 1989. The *Drosophila melanogaster l(2)gl* gene encodes a protein homologous to the cadherin cell-adhesion molecular family. *Dev. Biol.* 133:425–436.

Knudson, A. G. 1993. All in the (cancer) family. *Nature Genet.* 5:103–104.

Lane, N. J. 1992. Anatomy of the tight junction: invertebrates. *In* Tight Junctions. M. Cereijido, editor. CRC Press, Boca Raton, FL. 23–48.

Lewis, E. B. 1945. The relation of repeats to position effect in *Drosophila melanogaster. Genetics.* 36:137–166.

Lützelschwab, R., C. Klämbt, R. Rossa, and O. Schmidt. 1987. A protein product of the *Drosophila* recessive tumour gene *l(2)giant larvae*, potentially has cell adhesion properties. *EMBO (Eur. Mol. Biol. Organ.) J.* 6:1791–1797.

McCrea, P. D., and B. M. Gumbiner. 1991. Purification of a 92-kDa cytoplasmic protein tightly associated with the cell-cell adhesion molecule E-cadherin (Uvomorulin). *J. Biol. Chem.* 266:4515–4520.

McCrea, P. D., C. W. Turck, and B. Gumbiner. 1991. A homology of the armadillo protein in *Drosophila* (Plakoglobin) associated with E-Cadherin. *Science (Wash. DC).* 254:1359–1361.

Mechler, B. M. 1991. The fruitfly *Drosophila* and the fish *Xiphophorus* as model systems for cancer studies. *Cancer Surv.* 9:505–527.

Mechler, B. M., and T. H. Rabbitts. 1981. Membrane-bound ribosomes of myeloma cells IV. mRNA complexity of free and membrane-bound polysomes. *J. Cell Biol.* 88:29–36.

Mechler, B. M., and D. Strand. 1990. Tumour suppression in *Drosophila. In* Tumour Suppressor Genes. Immunological Series. Vol. 51. George Klein, editor. Marcel Dekker, Inc., New York. 123–144.

Mechler, B. M., W. McGinnis, and W. J. Gehring. 1985. Molecular cloning of *lethal(2)giant larvae*, a recessive oncogene of *Drosophila melanogaster. EMBO (Eur. Mol. Biol. Organ.) J.* 4:1551–1557.

Merz, R., M. Schmidt, I. Török, U. Protin, G. Schuler, H. P. Walther, F. Krieg, M. Gross, D. Strand, and B. M. Mechler. 1990. Molecular action of the *l(2)gl* tumour suppressor gene of *Drosophila melanogaster. Env. Health Persp.* 88:163–167.

Miller, A. 1950. The internal anatomy and histology of imago of *Drosophila melanogaster. In* Biology of *Drosophila.* M. Demerec, editor. Hafner Publishing Co., New York/London. 420–534.

Nagafuchi, A., and M. Takeichi. 1988. Cell binding function of E-cadherin is regulated by the cytoplasmic domain. *EMBO (Eur. Mol. Biol. Organ.) J.* 7:3679–3684.

Noirot-Timothee, C., and C. Noirot. 1980. Septate and scalariform junctions

in arthropods. *Int. Rev. Cytol.* 63:97–140.

O'Reilly, D. R., L. K. Miller, and V. A. Luckow. 1992. Baculovirus Expression Vectors: A Laboratory Manual. W. H. Freeman and Company, New York. 1–347.

Peifer, M. S. 1993. The product of the *Drosophila* segment poarity gene *armadillo* is part of a multi-protein complex resembling the vertebrate adherens junctions. *J. Cell Sci.* 105:993–1000.

Peifer, M., S. Orsulic, D. Sweeton, and E. Wischaus. 1993. A role for the *Drosophila* segment polarity gene *armadillo* in cell adhesion and cytoskeletal integrity during oogenesis. *Development.* 118:1191–1207.

Pesacreta, T. C., T. M. Byers, R. Dubreuil, D. P. Kiehart, and D. Branton. 1989. *Drosophila* spectrin: the membrane skeleton during embryogenesis. *J. Cell Biol.* 108:1697–1709.

Poodry, C. A. 1990. *shibire*, a neurogenic mutant of *Drosophila. Dev. Biol.* 138:464–472.

Poodry, C. A., and L. Edgar. 1979. Reversible alterations in the neuromuscular junctions of *Drosophila melanogaster* bearing a temperature-sensitive mutation, *shibire. J. Cell Biol.* 81:520–527.

Raska, I., R. L. Ochs, and L. Salamin-Michel. 1990. Immunocytochemistry of the cell nucleus. *Electron Microsc. Rev.* 3:301–353.

Rubinfeld, B., B. Souza, I. Albert, O. Müller, S. H. Chamberlain, and P. Polakis. 1993. Association of the *APC* gene product with β-catenin. *Science (Wash. DC).* 262:1731–1734.

Ryerse, J. S., and B. A. Nagel. 1984. Gap junction distribution in the *Drosophila* wing discs mutants *vg, l(2)gd, l(3)c43Hs1, and l(2)gl⁴. Dev. Biol.* 105:396–403.

Scharrer, B., and E. Hadorn. 1938. The structure of the ring-gland (corpus allatum) in normal and lethal larvae of *Drosophila melanogaster. Proc. Natl. Acad. Sci. USA.* 24:236–242.

Stewart, M. J., and R. Denell. 1993. Mutations in the 5'region of the *Drosophila* gene encoding ribosomal protein S6 are associated with tissue overgrowth. *Mol. Cell. Biol.* 13:2524–2535.

Strand, D., R. Jakobs, G. Merdes, B. Neumann, A. Kalmes, H. W. Heid, I. Husmann, and B. M. Mechler. 1994. The *Drosophila lethal(2)giant larvae* tumour suppressor protein forms homo-oligomers and is associated with nonmuscle myosin II heavy chain. *J. Cell Biol.* 127:1361–1373.

Su, L.-K., B. Vogelstein, and K. W. Kinzler. 1993. Association of the APC tumor suppressor protein with catenins. *Science (Wash. DC).* 262:1734–1737.

Summers, M. D., and G. E. Smith. 1988. A Manual of Methods for Baculovirus Vectors and Insect Cell Culture Procedures. Texas Agricultural Experiment Station Bulletin No. 1555. Texas Experimental Station, College Station, TX. 1–57.

Szabad, J., V. Jursnich, and P. J. Bryant. 1991. Requirement for cell-proliferation control genes in *Drosophila* oogenesis. *Genetics.* 127:525–533.

Tepass, U., and V. Hartenstein. 1994. The development of cellular junctions in the *Drosophila* embryo. *Dev. Biol.* 161:563–596.

Theurkauf, W. E., S. Smiley, M. L. Wong, and B. M. Alberts. 1992. Reorganization of the cytoskeleton during *Drosophila* oogenesis: implications for axis specification and intercellular transport. *Development.* 115:923–936.

Timmons, L., E. Hersperger, E. Woodhouse, J. Xu, L. Liu, and A. Shearn. 1993. The expression of the *Drosophila awd* gene during normal development and in neoplastic tumors caused by *lgl* mutations. *Dev. Biol.* 158:364–379.

Tokuyasu, K. T. 1986. Application of cryoultramicrotomy to immunocytochemistry. *J. Microsc.* 143:139–149.

Tomotsune, D., H. Shoji, Y. Wakamatsu, H. Kondoh, and N. Takahashi. 1993. A mouse homologue of the *Drosophila* tumour-suppressor gene *l(2)gl* controlled by Hox-C8 *in vivo. Nature (Lond.).* 365:69–72.

Török, I., K. Hartenstein, A. Kalmes, R. Schmitt, D. Strand, and B. M. Mechler. 1993a. The *l(2)gl* homologue of *Drosophila pseudoobscura* suppresses tumorigenicity in transgenic *Drosophila melanogaster. Oncogene.* 8:1537–1549.

Török, T., G. Tick, M. Alvarado, and I. Kiss. 1993b. *P-lacW* insertional mutagenesis on the second chromosome of *Drosophila melanogaster*: isolation of lethals with different overgrowth phenotypes. *Genetics.* 135:71–80.

Trofatter, J. A., M. M. MacCollin, J. L. Rutter, J. R. Murrell, M. P. Buyao, D. M. Parry, R. Eldridge, N. Kley, A. G. Menon, K. Pulaski, V. H. Haase, C. M. Ambrose, et al. 1993. A novel Moesin-, Ezrin- Radixin-like gene is a candidate for the neurofibromatosis 2 tumor suppressor. *Cell.* 72:791–800.

Tsukita, S., K. Oishi, T. Akiyama, Y. Yamanashi, T. Yamamoto, and S. Tsukita. 1991. Specific proto-oncogenic tyrosine kinases of src family are enriched in cell-to-cell adherens junctions where the level of tyrosine phosphorylation is elevated. *J. Cell Biol.* 113:867–879.

Tsukita, S., M. Itoh, A. Nagafuchi, S. Yonemura, and S. Tsukita. 1993. Submembrane junctional plaque proteins include potential tumor suppressor molecules. *J. Cell Biol.* 123:1049–1053.

van der Bliek, A. M., and E. M. Meyerowitz. 1991. Dynamin-like protein encoded by the *Drosophila shibire* gene associated with phosphorylation on assembly of adherens-type junctions. *EMBO (Eur. Mol. Biol. Organ.) J.* 11:1733–1742.

Volberg, T., Y. Zick, R. Dror, I. Sabanay, C. Gilon, A. Levitzki, and B. Geiger. 1992. The effect of tyrosine-specific protein phosphorylation on assembly of adherens-type junctions. *EMBO (Eur. Mol. Biol. Organ.) J.* 11:1733–

1742.

Warn, R. M., and M. Robert-Nicoud. 1990. F-actin organization during the cellularization of the *Drosophila* embryo as revealed with a confocal laser scanning microscope. *J. Cell Sci.* 96:35–42.

Watson, K. L., K. D. Konrad, D. R. Woods, and P. J. Bryant. 1992. *Drosophila* homolog of the human S6 ribosomal protein is required for tumor suppression in the hematopoietic system. *Proc. Natl. Acad. Sci. USA.* 89: 11302–11306.

Welch, R. M. 1957. A developmental analysis of the lethal mutant *l(2)gl* of *Drosophila melanogaster* based on cytophotometric determination of nuclear desoxyribonucleic acid (DAN) content. *Genetics.* 42:544–545.

Wiegant, F. A. C., F. J. Block, L. H. K. Defize, W. A. M. Linnemans, A. J. Verkley, and J. Boonstra. 1986. Epidermal growth factor receptors associated to cytoskeletal elements of epidermoid carcinoma (A431) cells. *J. Cell Biol.* 103:87–94.

Woods, D. F., and P. J. Bryant. 1991. The *discs-large* tumor suppressor gene of *Drosophila* encodes a guanlyate kinase homolog localized at septate junctions. *Cell.* 66:451–464.

Woodhouse, E., E. Hersperger, W. Stetler-Steveson, L. Liotta, and A. Shearn. 1994. Increased type IV collangenase in *lgl*-induced invasive tumors of *Drosophila. Cell Growth and Differentiation.* 5:151–159.

Young, P.E., T. C. Pesacreta, and D. P. Kiehart. 1991. Dynamic changes in the distribution of cytoplasmic myosin during *Drosophila* embryogenesis. *Development.* 111:1–14.